

Anisotropic exchange interactions in CuTe₂O₅

R. M. Eremina, T. P. Gavrilova, Hans-Albrecht Krug von Nidda, Andrei Pimenov, Joachim Deisenhofer, Alois Loidl

Angaben zur Veröffentlichung / Publication details:

Eremina, R. M., T. P. Gavrilova, Hans-Albrecht Krug von Nidda, Andrei Pimenov, Joachim Deisenhofer, and Alois Loidl. 2008. "Anisotropic exchange interactions in CuTe₂O₅." *Physics of the Solid State* 50 (2): 283–89. <https://doi.org/10.1134/s106378340802011x>.

Nutzungsbedingungen / Terms of use:

licgercopyright

Dieses Dokument wird unter folgenden Bedingungen zur Verfügung gestellt: / This document is made available under these conditions:

Deutsches Urheberrecht

Weitere Informationen finden Sie unter: / For more information see:

<https://www.uni-augsburg.de/de/organisation/bibliothek/publizieren-zitieren-archivieren/publiz/>



Anisotropic Exchange Interactions in CuTe_2O_5

R. M. Eremina^a, T. P. Gavrilova^b, N.-A. Krug von Nidda^c, A. Pimenov^c,
J. Deisenhofer^d, and A. Loidl^c

^a *Zavoiskii Physicotechnical Institute, Kazan Scientific Center, Russian Academy of Sciences,
Sibirskii trakt 10/7, Kazan 29, 420029 Tatarstan, Russia*

e-mail: R Eremina@yandex.ru

^b *Kazan State University, ul. Kremlevskaya 18, Kazan, 420008 Tatarstan, Russia*

^c *Institute for Physics, Augsburg University, Augsburg, D-86135 Germany*

^d *Département de Physique de la Matière Condensée, Université de Geneva, Geneva 4, CH-1211 Switzerland*

Abstract—Electron paramagnetic resonance (EPR) was used to study CuTe_2O_5 single crystals at frequencies of 9.4 and 160 GHz. Analytic expressions for the second and fourth moments of the EPR line are deduced with inclusion of the difference between the exchange couplings of the copper spin with its different neighbors. From comparing the calculated and measured EPR linewidths, the positions of copper ions with the strongest exchange interactions are identified. The parameters of the anisotropic exchange interaction between copper ions in a pair are found. The parameter of the exchange interaction between magnetically nonequivalent copper centers is determined from the frequency dependence of the EPR linewidth. The directions of the principal axes of the g tensors are established. The data obtained count in favor of a quasi-one-dimensional model of magnetism in CuTe_2O_5 .

1. INTRODUCTION

Observation of the spin-Peierls transition in CuGeO_3 [1] has stimulated searches of similar low-dimensional materials. Lemmens et al. [2] found that, as the temperature decreases, the magnetic susceptibility of CuTe_2O_5 , as well as that of CuGeO_3 , decreases along the three crystallographic directions. An analysis of the structural data allows the assumption that the dimerization of copper spins occurs in CuTe_2O_5 ; i.e., as in the case of CuGeO_3 , dimers with a singlet ground state are formed. The crystalline structure of CuTe_2O_5 belongs to space group $P2_1/c$. The unit cell consists of four formula units, and its dimensions are $a = 6.871$ Å, $b = 9.322$ Å, $c = 7.602$ Å; the angle β between the a and c axes is 109.08° [3]. There are four nonequivalent positions of copper ions in the unit cell. The Cu(1)–Cu(2) and Cu(3)–Cu(4) distances between neighboring copper ions are 3.18 Å; these pairs form structural dimers. Upon translation of the Cu(1) and Cu(3) positions along the c axis, the Cu'(1)–Cu(2) and Cu'(3)–Cu(4) bond lengths are 5.585 Å. The Cu(1)–Cu(3) distance is 5.28 Å. Each of the copper ions is surrounded by six oxygen atoms forming a strongly distorted octahedron. The copper ion is positioned at a distance of 1.95 Å from oxygen ion O5, at 1.961 Å from O4, at 1.953 Å from O1, and at 1.969 Å from O3; oxygen O5' is positioned at a distance of 2.303 Å from the copper ion and is oxygen O5 for a neighboring octahedron

(Fig. 1). Two edge-shared octahedra containing Cu(1)–Cu(2) or Cu(3)–Cu(4) at their centers determine the magnetic properties of the material. The octahedra of the Cu(1)–Cu(2) or Cu(3)–Cu(4) neighboring pairs are rotated relative to each other and are magnetically nonequivalent. The Te^{4+} cations connect the copper–oxygen octahedra together. The magnetic susceptibility of CuTe_2O_5 exhibits a maximum at a temperature of 56.6 K. By fitting the temperature dependence of the magnetic susceptibility at high temperatures, one can determine the Curie temperature to be $\theta = -41$ K.

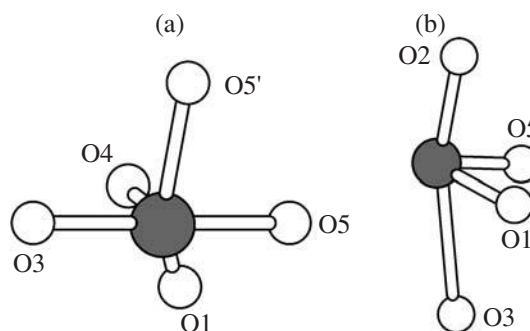


Fig. 1. Local structures of fragments (a) CuO_5 and (b) TeO_4 in CuTe_2O_5 .

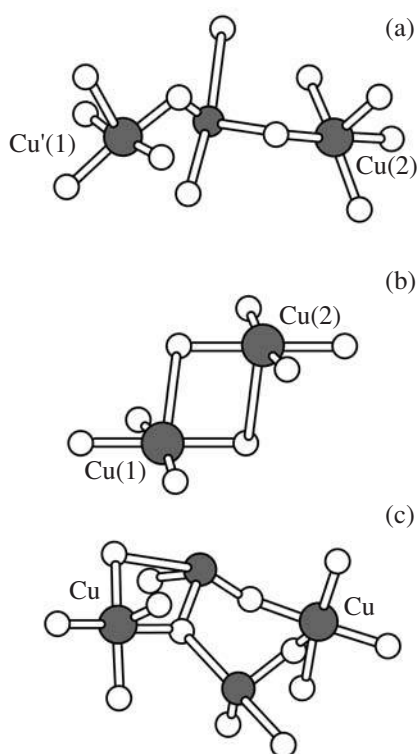


Fig. 2. Structures of pairs of copper and oxygen ions with bridge fragments TeO_4 for pairs (a) 4, (b) 1, and (c) 5 [4].

In [4], several approaches were used to describe the temperature dependence of the magnetic susceptibility of CuTe_2O_5 . The experimental results are best described in terms of the following two models. One is a model of a quasi-one-dimensional antiferromagnetic spin chain with alternating exchange interactions J_1 and J_2 . Fitting of the experimental data gives $J_1 = 93.3$ K and $J_2 = 40.7$ K. In another model, the magnetic susceptibility is calculated using a modified Bleaney–Bowers

Table 1. Calculated exchange interactions J_i [4] and hopping integrals t_i^2 [5] (in arbitrary units) for Cu–Cu pairs in CuTe_2O_5

No.	$R_{\text{Cu-Cu}}, \text{\AA}$	J_i/J_6 [4]	$(t_i/t_4)^2$ [5]
1	3.187	0.59	0.12
2	5.282	0.05	–
3	5.322	0.14	0.01
4	5.585	0.11	1
5	5.831	0.01	0.015
6	6.202	1	0.28
7	6.437	0.05	0.002
8	6.489	0.09	–
9	6.871	0.26	–

equation in the mean-field approximation. Fitting of the temperature dependence of the magnetic susceptibility gives other parameter values of the isotropic exchange interaction between copper spins; namely, presumably within the dimer, $J = 88.9$ K and, between the spins of copper ions of neighboring dimers, $J' = 91.4$ K. Which of the variants considered in [4] is more preferable remained unclear. Moreover, it is unclear to which pair of copper ions one should assign the parameter of the exchange interaction equal to 90 K. In [4], the parameters of the isotropic exchange interaction for different pairs were calculated by the EHTB method. It turned out that, for copper pairs in a structural dimer separated by a distance of 3.18 Å (Fig. 2b), the calculated parameter of this interaction ($J_a \sim 54$ K) is approximately half the value obtained by fitting (~ 90 K); this result casts doubt on the conclusion that this pair is dimerized. The arrangement of the copper and oxygen ions in the structural dimer is shown in Fig. 2b. According to the calculations performed in [4], the indirect exchange interaction is the strongest for the spins of copper ions coupled via oxygen and tellurium ions (Fig. 2a), rather than for pairs of nearest neighboring ions. The authors of [5] used another (NMTD) method to calculate the hopping integrals for different pairs of copper ions in CuTe_2O_5 . Table 1 lists the data from [4, 5]. The pairs are numbered in order of increasing distance between copper ions. The third column presents the calculated values of the exchange integrals (in arbitrary units) taken from [4]. The fourth column presents the squared hopping integrals calculated in [5] (in arbitrary units) for different copper ion pairs in the CuTe_2O_5 single crystal. It is generally believed [6] that the strength of isotropic exchange interaction is proportional to the square of the transfer integral. From Table 1, it is seen that, according to [5], the strongest interaction should be expected for pairs of the fourth-nearest neighbors rather than for sixth neighbors as was concluded in [4]. Taking the data from [4], we obtain the quasi-one-dimensional model of magnetism for CuTe_2O_5 ; for data from [5], a two-dimensional dimerization is realized in CuTe_2O_5 . The conclusions concerning the electron structure are qualitatively different, and it is necessary to obtain additional experimental information. This circumstance stimulated our study of CuTe_2O_5 single crystals by the EPR method. This method makes it possible to determine immediately the parameter of isotropic exchange between magnetically nonequivalent spins from the frequency spectrum, which is made in this work. Moreover, we obtained additional information on the anisotropic exchange interactions from analyzing the angular dependence of the EPR linewidth in three mutually perpendicular planes.

2. EXPERIMENTAL

We studied a $0.2 \times 1 \times 1$ -mm CuTe_2O_5 single crystal, which was transparent and sea-green in color. This

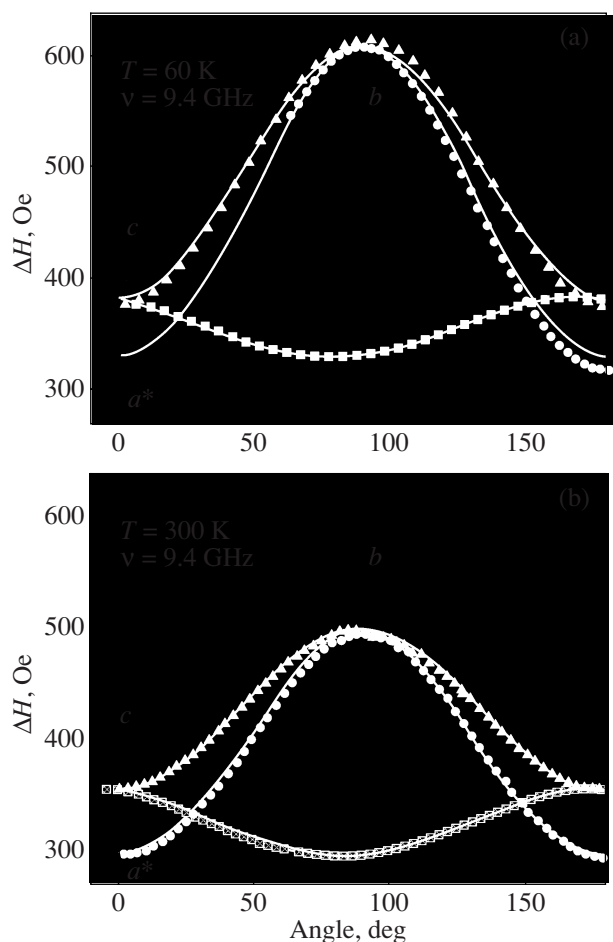


Fig. 3. Angular dependences of the EPR linewidth in CuTe_2O_5 at a frequency of 9.4 GHz in the crystallographic planes a^*b (circles), bc (triangles), and a^*c (squares) measured at temperatures of (a) 60 and (b) 300 K. Solid lines are theoretical calculations.

sample was presented by Lemmens (Braunschweig University, Germany). The EPR spectra were measured using a Bruker Elexsys E500 CW spectrometer in several frequency ranges at temperatures of 5 to 300 K. In the high-frequency range, the EPR spectra were measured using quasi-optic methods. At temperatures of 25 to 300 K, the EPR spectrum of copper ions consists of one Lorentzian-shaped line with $g \sim 2$. The temperature dependence of the integrated EPR line intensity follows that of the magnetic susceptibility; i.e., the intensity of the Lorentzian-shaped line decreases as the temperature decreases. Near 25 K, the line splits into several components. We associate the appearance of these signals in the EPR spectrum with the presence of defects in the CuTe_2O_5 crystal, which prevent a part of copper ion pairs from being dimerized. The specific features of the structure of single paramagnetic centers revealed in the EPR spectrum at low temperatures are not discussed in this work. We concentrate most attention on the exchange-narrowed EPR line of copper ions in

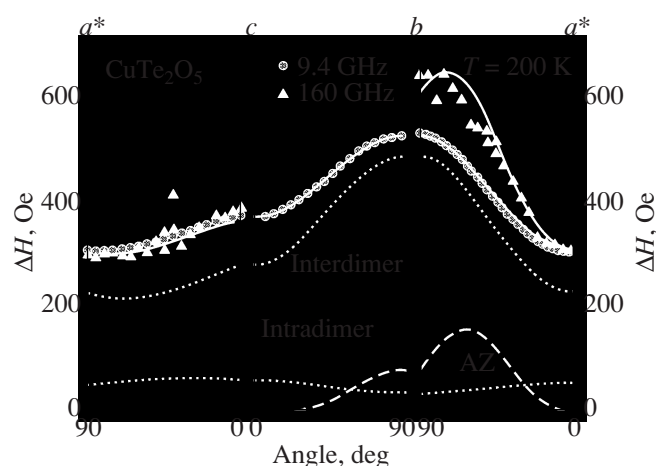


Fig. 4. Angular dependences of the EPR linewidth in CuTe_2O_5 at frequencies of 9.4 (circles) and 160 GHz (triangles) in three crystallographic planes measured at $T = 200$ K. The dotted lines show the contribution to the EPR linewidth from the spin-spin interactions between copper ions in a dimer and between copper ions belonging to neighboring dimers. The dashed line corresponds to the contribution from the anisotropic Zeeman effect at 160 GHz. The solid lines show the sum of all the contributions (for each frequency).

CuTe_2O_5 at high temperatures. The angular dependence of the width of this line was measured at temperatures of 60 and 300 K in the X band and at 200 K at frequencies of 9.4 and 160 GHz. Figures 3 and 4 show the experimental data on the EPR linewidth measured in three mutually perpendicular planes: a^*b , ac , and bc , where the a^* axis is perpendicular to the crystallographic b and c axes. As the temperature decreases, the EPR linewidth increases significantly when the magnetic field is applied along the b axis and it remains practically unchanged when the magnetic field is oriented along the a^* or c axis. In the EPR spectrum measured at a high frequency, an abrupt increase in the EPR linewidth occurs only when the magnetic field is applied along the b axis of the crystal. The angular dependence of the g factor for the EPR line measured in three mutually perpendicular planes of CuTe_2O_5 are shown in Fig. 5. The anisotropy of the position of this line is practically independent of the frequency and temperature at which the experiment was performed.

3. CALCULATION OF THE SECOND AND FOURTH MOMENTS OF THE EPR LINE

The theory of the EPR linewidth for exchange-coupled systems has been well developed [7]. In compounds with a fairly strong exchange interaction, the EPR line shape is close to a Lorentzian and its width

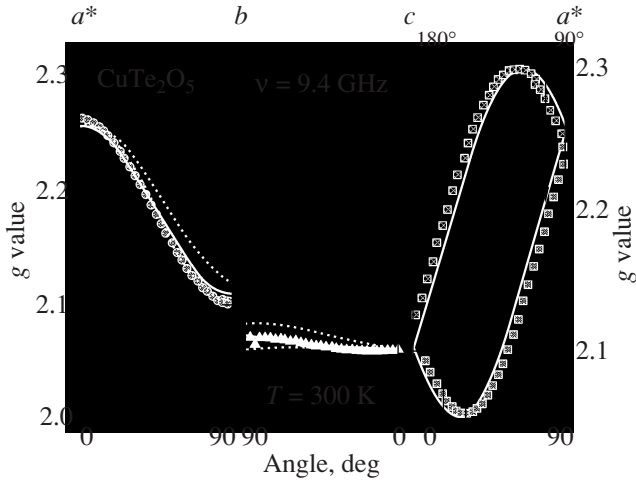


Fig. 5. Angular dependences of the position of the EPR line from CuTe_2O_5 in the X band in the crystallographic planes a^*b (circles), bc (triangles), and a^*c (squares) measured at $T = 300$ K. The dotted lines show the angular dependences of the EPR line position separately for each of the two magnetically nonequivalent ions. The solid line is theoretical calculation.

ΔH can be expressed in terms of the second (M_2) and fourth (M_4) moments of the line as follows:

$$\Delta H = \frac{\pi}{\sqrt{3}} \left(\frac{M_2^3}{M_4} \right)^{1/2}. \quad (1)$$

In a high-temperature approximation ($kT \gg J$), calculations of the second and fourth moments are fairly simple and ΔH can be expressed in terms of the microscopic parameters of the Hamiltonian of the spin system. In this case, it is generally assumed that the exchange interactions of a spin with its nearest neighbors on the left and those on the right are identical. In our case, this assumption is very rough. In what follows, we use the spin Hamiltonian

$$H = J_{1a}(S_1 S_a) + \sum_{\alpha, \beta = x, y, z} J_{1a}^{\alpha\beta} S_1^\alpha S_a^\beta + J_{1b}(S_1 S_b) + \sum_{\alpha, \beta = x, y, z} J_{1b}^{\alpha\beta} S_1^\alpha S_b^\beta + J_{1c}(S_1 S_c) + \sum_{\substack{\alpha, \beta = x, y, z \\ \gamma = 1-3}} g_\gamma^{\alpha\beta} \mu_B H_\gamma S_\gamma^\alpha S_\gamma^\beta. \quad (2)$$

In this model spin Hamiltonian, we included isotropic and anisotropic exchange interactions between three types of ions: J_{1a} is the parameter of the isotropic exchange interaction with the largest magnitude for copper ion pair 1; J_{1b} is the parameter of the isotropic exchange interaction for the same pair with the strength next in magnitude; J_{1c} , the isotropic exchange interaction between magnetically nonequivalent systems formed by copper ions; and the last term describes the interaction with the magnetic field. We note that the

summation over all $\text{Cu}(1)$ positions in Eq. (2) is dropped for brevity.

Not specifying a model of chains, we only assume that $J_{1c} \ll J_{1a}$ and $J_{1c} \ll J_{1b}$. The EPR line moments were calculated using a standard technique described, e.g., in [7]. In a coordinate system with the z axis directed along the external magnetic field, the second and fourth moments of the EPR line are given by

$$M_2(J) = \frac{2S(S+1)}{3} (B(J_{1a}) + B(J_{1b})), \quad (3)$$

$$M_4 = \frac{a(6a-7)}{30} (J_{1a}^2 B(J_{1a}) + J_{1b}^2 B(J_{1b})) + \frac{a^2}{9} (J_{1b}^2 B(J_{1a}) + J_{1a}^2 B(J_{1b})) + \frac{a^2 J_{1a} J_{1b}}{9} ((2J_{1a}^{zz} - J_{1a}^{xx} - J_{1a}^{yy})(2J_{1b}^{zz} - J_{1b}^{xx} - J_{1b}^{yy}) + (J_{1a}^{xx} - J_{1a}^{yy})(J_{1b}^{xx} - J_{1b}^{yy}) + 10J_{1a}^{xz} J_{1b}^{xz} + 10J_{1a}^{yz} J_{1b}^{yz} + 4J_{1a}^{xy} J_{1b}^{xy}),$$

where $a = S(S+1)$ and $B(J_{1a}) = (2J_{1a}^{zz} - J_{1a}^{xx} - J_{1a}^{yy})^2 + (J_{1a}^{xx} - J_{1a}^{yy})^2 + 10(J_{1a}^{xz})^2 + 10(J_{1a}^{yz})^2 + 4(J_{1a}^{xy})^2$. The function $B(J_{1b})$ is similar in form to $B(J_{1a})$ but it includes anisotropic symmetric exchange interactions between copper spins of neighboring dimers. The functions $J_{1\gamma}^{\alpha\beta}$ (where $\alpha, \beta = x, y, z$; and $\gamma = a, b$) as expressed in terms of the parameters of the anisotropic symmetric exchange with respect to the crystallographic axes can be found in [8]. In the specific case $J_{1a} = J_{1b} = J$ and $J^{\alpha\beta} = J_{1b}^{\alpha\beta}$, for particles with spin $S = 1/2$, the expression for the fourth moment simplifies to

$$M_4 = \frac{a^2 J^2}{9} ((2J_{zz} - J_{xx} - J_{yy})^2 + (J_{xx} - J_{yy})^2 + 10J_{xz}^2 + 10J_{yz}^2 + 4J_{xy}^2). \quad (5)$$

From comparing the angular dependences of the EPR linewidth calculated from Eq. (1) with the experimental ones, we can obtain information on the parameters $J_{1a}^{\alpha\beta}$, $J_{1b}^{\alpha\beta}$, and J_{1c} .

4. DETERMINATION OF THE PARAMETERS OF THE SPIN HAMILTONIAN

The angular dependences of the EPR linewidth of CuTe_2O_5 calculated theoretically and measured at frequencies of 9.4 and 160 GHz at $T = 200$ K are presented in Fig. 4. As noted above, the EPR linewidth along the b axis at a frequency of 160 GHz is greater than its value in the X band. It is logical to assume that this is

associated with the difference between the g factors of interacting spins (anisotropic Zeeman effect). Indeed, from analyzing the structural data, it follows that the unit cell contains two magnetically nonequivalent octahedra of oxygen ions that surround the paramagnetic copper ions producing an EPR signal. Since the EPR spectrum exhibits one line, its effective g factor is the average of the g factors of two copper centers located in nonequivalent positions. The frequency-dependent contribution to the EPR linewidth due to the difference between the g factors [9] is given by

$$\Delta H_{AZ} = \left(\frac{\Delta g}{g} \right)^2 \frac{g \mu_B H_{\text{res}}^2}{J_{1c}}, \quad (6)$$

where Δg is the difference between the g factors of the nonequivalent paramagnetic centers. Prior to analyzing the g factors, we note that the resonance frequency is related to the resonance magnetic field by the equation $g\beta H_{\text{res}} = h\nu_{\text{res}}$. Using the values of Δg and ΔH_{AZ} determined from the experimental data, we can find J_{1c} from Eq. (6).

The angular dependence of the EPR linewidth measured at 160 GHz shows that the difference between the g factors of the two nonequivalent octahedra is maximum along the b axis of the crystal and is minimum along the other directions. Since the geometric sizes of the two magnetically nonequivalent octahedra are equal, the principal values of the g tensors in a local coordinate system of the octahedra also have to be equal. Based on this conclusion, we analyzed the experimental angular dependences of the g factors and the EPR linewidth at 160 GHz measured at 200 K. When fitting the experimental values of the EPR linewidth obtained at 160 GHz, we took into account that the contribution from the anisotropic symmetric interactions is the same as that in the X band. The analysis showed that the experimental angular dependences of the position and width of the EPR line at 160 GHz are described fairly well by the following g tensors of the two magnetically nonequivalent centers: $g(1) = \{2.055, 2.10, 2.30\}$ and $g(2) = \{2.056, 2.12, 2.30\}$. To within one degree, the directions of the principal axes are as follows:

$$\begin{pmatrix} -0.4289 & 0.0093 & -0.9033 \\ 0.0554 & 0.9983 & -0.0161 \\ 0.9017 & -0.0569 & -0.4287 \end{pmatrix}$$

and

$$\begin{pmatrix} -0.4278 & -0.0252 & 0.9035 \\ -0.0523 & -0.9972 & -0.0526 \\ 0.9024 & -0.0698 & 0.4253 \end{pmatrix}.$$

The axis along which the principal value of the g tensor is maximum coincides with the Cu–O5' direction, and

the other two principal axes of the g tensor lie in the basal plane of the CuO_6 octahedron; specifically, one of them is perpendicular to the O1–O3 bond and the other is perpendicular to the O1–O5 bond. The isotropic exchange interaction between the spins of the copper ions belonging to neighboring magnetically nonequivalent octahedra as estimated from Eq. (6) is $J_{1c} = 0.5$ K. The theoretically calculated isotropic exchange interaction for pair 5 (Table 1) is about 0.7 K, which almost coincides with the value obtained from the experimental data.

In [10, Eqs. (7.110)], the principal values of the g tensor of ions of d^9 configuration in octahedral surroundings in the case of trigonal distortions due to the Yang–Teller effect are given to be

$$\begin{aligned} g_1 &= 2 - \frac{2\lambda}{\Delta} \left(\cos \frac{1}{2}\varphi - \sqrt{3} \sin \frac{1}{2}\varphi \right)^2, \\ g_2 &= 2 - \frac{2\lambda}{\Delta} \left(\cos \frac{1}{2}\varphi + \sqrt{3} \sin \frac{1}{2}\varphi \right)^2, \\ g_3 &= 2 - \frac{8\lambda}{\Delta} \cos^2 \frac{1}{2}\varphi, \end{aligned} \quad (7)$$

where λ/Δ is the ratio of the spin–orbital interaction strength to the spacing between the ground and excited states. The eigenfunction of the ground state is

$$\cos \frac{1}{2}\varphi |x^2 - y^2\rangle + \sin \frac{1}{2}\varphi |3z^2 - r^2\rangle. \quad (8)$$

From analyzing the obtained principal values of the g tensor in CuTe_2O_5 , it follows that $-\lambda/\Delta = 0.038$ and $\cos \frac{1}{2}\varphi \approx 0.99$. In this case, the eigenfunction of the ground state of the copper ion is $|x^2 - y^2\rangle$ and is localized in the basal plane of the octahedron (O1–O3–O5–O4). The experimental angular dependences of the g factor are described very well by the theoretical curves (Fig. 5).

Let us consider a possibility of describing the angular dependence of the EPR linewidth in CuTe_2O_5 at a frequency of 9.4 GHz in terms of two models, namely, EHTB [4] and NMTO [5].

According to [4], the exchange interaction is maximum in pair 6. In this pair, the Cu(1)–Cu(4) copper ions positioned in the bc plane are bonded. The Cu(1)–Cu(4) and Cu(2)–Cu(3) directions form an angle of about 37° with the b axis. Next in magnitude is expected to be the bonding in pair 1, which lies in the ac plane. These two pairs can form a unit cell of the exchange-coupled system. An analysis of the angular dependence of the EPR linewidth in terms of this model suggests that the EPR linewidth should reach a maximum in the case where the magnetic field is applied at an angle of 37° to the b axis in the bc plane, which corresponds to the bond direction of pair 6. Such behavior is in contradiction with the experimental data obtained in the X band. Gen-

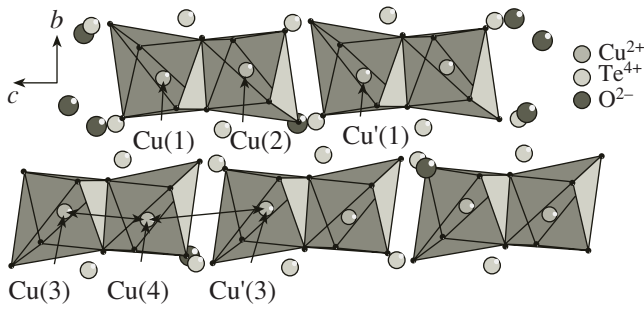


Fig. 6. Quasi-one-dimensional chain formed by copper ions Cu(1)–Cu(2)–Cu'(1) and Cu(3)–Cu(4)–Cu'(3) in the bc plane.

erally speaking, a misalignment of the directions of the experimental extreme values of the EPR linewidth (or g factor) with the crystallographic axes is possible. However, it usually takes place in crystals with monoclinic symmetry [9]. In the CuTe_2O_5 crystal, such misalignment of the direction of extreme values of the g factor is observed in the ac plane (Fig. 5).

Another possible model for describing the angular dependence of the EPR linewidth is based on the results obtained in [5]. The maximum exchange interaction is expected in pair 4. However, in this case, the directions of the principal axes of the tensor of the anisotropic exchange interactions in pair 4 are such that we fail to describe all specific features of the angular dependence of the EPR linewidth. For example, if pairs 4 and 6 are a translation element, then this model fails to explain the behavior of the EPR linewidth in the bc plane.

It is most probable that the building block of the exchange-coupled system consists of pairs 1 (Cu(1)–Cu(2)) and 4 (Cu'(1)–Cu(2)). The structural positions of the copper ions are as follows: Cu(1)[x , y , z]–Cu(2)[$\bar{x} + 1$; $\bar{y} + 1$, $\bar{z} + 1$]–Cu'(1)[x ; y ; $z + 1$], where $x = 0.34117$, $y = 0.48715$, and $z = 0.29408$ [3]. It should be noted that the value $\bar{y} + 1 = 0.51285$ almost coincides with y , which means that Cu(1)–Cu(2)–Cu'(1) nearly coincides with the ac plane. The chain is formed upon translation along the c axis. The copper ions Cu(3)[$\bar{x} + 1$; $y + 0.5$, $\bar{z} + 0.5 + 1$]–Cu(4)[x ; $\bar{y} + 0.5 + 1$; $z + 0.5$]–Cu'(3)[$\bar{x} + 1$; $y + 0.5$; $\bar{z} + 0.5$] form another chain, which is magnetically nonequivalent to the chain

Cu(1)–Cu(2)–Cu'(1) and is shifted with respect to it by $b/2$ (Fig. 6).

This model allows one to explain satisfactorily all specific features of the EPR line in CuTe_2O_5 .

The anisotropic symmetric exchange interaction is known to be proportional to the deviation of the tensor component $g_{\alpha\alpha}$ from 2; namely, $(J_{\alpha\alpha} = [(g_{\alpha\alpha} - 2)/g_{\alpha\alpha}]^2 J)$. Moreover, it is seen that the principal values of the tensor of the anisotropic symmetric exchange interaction J_{α} are maximum for ion pairs with the maximum J . Therefore, based on the data from [5], we assume that the main contribution to the EPR linewidth comes from the anisotropic exchange interactions within copper ion pairs 4 (Fig. 2a) and 1 (Fig. 2b). We note that there is no antisymmetric exchange interaction in a structural dimer, since this dimer is symmetric with respect to the interchange of the ions [11]. We analyzed the angular dependence of the EPR linewidth of the copper ions in the X band at temperatures of 60, 200, and 300 K using Eq. (2). Since the two models describing the temperature dependence of the magnetic susceptibility give practically the same maximum value of the isotropic exchange [4], we estimated the principal values of the anisotropic exchange tensor using the value $J_{1a} = 90$ K. We assume that this value of the isotropic exchange can be assigned to the copper ion pair shown in Fig. 2a. The isotropic exchange interaction within a structural-dimer pair is $J_{1b} = 0.12J \approx 11$ K [5]. By fitting the experimental angular dependence of the EPR linewidth at temperatures of 60, 200, and 300 K in the X band, we estimated the parameters of the symmetric anisotropic exchange within pairs 1 and 4 under the condition that $J_{1\gamma}^{x'x'} + J_{1\gamma}^{y'y'} + J_{1\gamma}^{z'z'} = 0$, where $\gamma = a, b$. The parameters of the anisotropic symmetric exchange interaction are listed in Table 2 in local coordinate systems $x'y'z'$ for pair 1 and $x''y''z''$ for pair 4. The theoretically calculated values of the EPR linewidth in three mutually perpendicular planes a^*b , a^*c , and bc at temperatures of 60, 200, and 300 K are presented in Figs. 3 and 4. At temperatures of 60, 200, and 300 K, the theoretical and experimental values of the EPR linewidth practically coincide. As the temperature increases from 60 to 200 K, the anisotropic exchange increases in pair 1 and decreases in pair 4. The direction of the axes of the anisotropic exchange interaction in the local coordinate system of copper pairs is determined as follows: the $z'(z'')$ axis coincides with the Cu–Cu direction in a pair, and the axes $x'(x'')$ and $y'(y'')$ lie in a plane perpendicular to this direction. The directions of the local axes of the anisotropic exchange interaction in the coordinate system a^*bc for the two magnetically nonequivalent pairs of copper ions are given by the matrix of direction cosines. For pair 1, we have

Table 2. Parameters of the anisotropic symmetric exchange interaction for copper ion spins in pairs 1 and 4 at various temperatures

T , K	$J_{1a}^{x''x''}$, K	$J_{1a}^{z''z''}$, K	$J_{1b}^{x'x'}$, K	$J_{1b}^{z'z'}$, K
60	–1	2.19	0.55	–0.33
200	–0.82	1.98	0.65	–0.42
300	–0.82	1.92	0.64	–0.42

$$\begin{pmatrix} -0.71 & 0.2773 & 0.6473 \\ -0.3025 & -0.9502 & 0.0752 \\ 0.6359 & -0.1424 & 0.7585 \end{pmatrix}$$

and

$$\begin{pmatrix} -0.71 & -0.2773 & 0.6473 \\ 0.3025 & -0.9502 & -0.0752 \\ 0.6359 & 0.1424 & 0.7585 \end{pmatrix},$$

for pair 4, we have

$$\begin{pmatrix} 0.929 & -0.0158 & -0.3696 \\ 0 & 0.999 & -0.0429 \\ 0.3699 & 0.0399 & 0.9283 \end{pmatrix}$$

and

$$\begin{pmatrix} 0.929 & 0.0158 & -0.3696 \\ 0 & 0.999 & 0.0429 \\ 0.3699 & -0.0399 & 0.9283 \end{pmatrix}.$$

All of these data agree well with the conclusion that there are two types of magnetically nonequivalent chains in the CuTe_2O_5 single crystal. In Fig. 6, these chains are $\text{Cu}(1)\text{--Cu}(2)\text{--Cu}'(1)$ and $\text{Cu}(3)\text{--Cu}(4)\text{--Cu}'(3)$. In the model proposed here, we combined the results of calculations performed in [4, 5]. The exchange parameters are (approximately) $J[\text{Cu}(1)\text{--Cu}(2)] = J[\text{Cu}'(3)\text{--Cu}(4)] = 11$ K in the structural dimer and $J[\text{Cu}'(1)\text{--Cu}(2)] = J[\text{Cu}'(3)\text{--Cu}(4)] = 90$ K in a pair. The interchain exchange parameter is 0.5 K.

5. CONCLUSIONS

The angular dependences of the g factors and of the EPR linewidth have been studied in detail in the CuTe_2O_5 single crystal at frequencies of 9.4 and 160 GHz. The directions of the local axes of the g tensor of two magnetically nonequivalent octahedra have been determined. We established the parameters of the symmetric anisotropic exchange interaction between the spins of copper ions within a structural dimer and

between the copper ion spins of neighboring dimers. The data obtained shows that there are two types of magnetically nonequivalent chains in CuTe_2O_5 . The values of the exchange coupling in chains are 90 and 11 K, and the interchain exchange parameter is 0.5 K.

ACKNOWLEDGMENTS

We are grateful to M.V. Eremin for useful discussions.

This work was supported by the Russian Foundation for Basic Research (project no. 06-02-17401) and Swiss NSF through the NCCR MaNEP.

REFERENCES

1. M. Hase, I. Terasaki, and K. Uchinokura, *Phys. Rev. Lett.* **70**, 3651 (1993).
2. P. Lemmens, G. Guntherodt, and C. Gros, *Phys. Rep.* **375**, 1 (2003).
3. K. Hanke, V. Kupcik, and O. Lindqvist, *Acta Crystallogr., Sect. B: Struct. Crystallogr. Cryst. Chem.* **29**, 963 (1973).
4. J. Deisenhofer, R. M. Eremina, A. Pimenov, T. Gavrilova, H. Berger, M. Johnsson, P. Lemmens, H.-A. Krug von Nodda, A. Loidl, K.-S. Lee, and M.-H. Whangbo, *Phys. Rev. B: Condens. Matter* **74**, 174421 (2006).
5. H. Das and T. Saha-Dasgupta, *cond-mat/0703675* (2007).
6. P. W. Anderson, *Solid State Phys.* **14**, 99 (1963).
7. S. A. Al'tshuler and B. M. Kozyrev, *Electron Paramagnetic Resonance* (Nauka, Moscow, 1961; Academic, New York, 1964).
8. R. M. Eremina, M. V. Eremin, V. N. Glazkov, H.-A. Krug von Nidda, and A. Loidl, *Phys. Rev. B: Condens. Matter* **68**, 014417 (2003).
9. M. Heinrich, H.-A. Krug von Nidda, A. Krimmel, A. Loidl, R. M. Eremina, A. D. Ineev, B. I. Kochelaev, A. V. Prokofiev, and W. Assmus, *Phys. Rev. B: Condens. Matter* **67**, 224418 (2003).
10. A. Abragam and B. Bleaney, *Electron Paramagnetic Resonance of Transition Ions* (Clarendon, Oxford, 1970; Mir, Moscow, 1972), Vol. 1.
11. A. S. Moskvina and I. G. Bostrem, *Fiz. Tverd. Tela (Leningrad)* **19** (9), 2616 (1977) [*Sov. Phys. Solid State* **19** (9), 1532 (1977)].

Translated by Yu. Ryzhkov